

## HIGHLY UNDERSATURATED ANIONS IN THE CRYSTAL STRUCTURE OF ANDYROBERTSITE – CALCIO-ANDYROBERTSITE, A DOUBLY ACID ARSENATE OF THE FORM $K(\text{Cd,Ca})[\text{Cu}^{2+}_5(\text{AsO}_4)_4\{\text{As}(\text{OH})_2\text{O}_2\}](\text{H}_2\text{O})_2$

MARK A. COOPER AND FRANK C. HAWTHORNE<sup>§</sup>

Department of Geological Sciences, University of Manitoba, Winnipeg, Manitoba R3T 2N2, Canada

### ABSTRACT

The crystal structure of andyrobetsite, ideally  $K\text{Cd}[\text{Cu}^{2+}_5(\text{AsO}_4)_4\{\text{As}(\text{OH})_2\text{O}_2\}](\text{H}_2\text{O})_2$ , monoclinic,  $a$  9.8102(9),  $b$  10.0424(6),  $c$  9.9788(7) Å,  $\beta$  101.686(7)°,  $V$  962.6(1) Å<sup>3</sup>,  $P2_1/m$ ,  $Z = 2$ , has been solved by direct methods and refined to an  $R$  index of 2.3% for 2140 observed ( $F_o > 5\sigma F$ ) reflections measured with  $\text{MoK}\alpha$  X-radiation. There are three crystallographically distinct  $As$  sites, each occupied by  $\text{As}^{5+}$  in tetrahedral coordination. One of the  $As$  sites is coordinated by two O atoms and two (OH) groups to form a doubly acid arsenate group,  $\{\text{As}(\text{OH})_2\text{O}_2\}$ . There are four crystallographically distinct  $Cu$  sites, each occupied by  $\text{Cu}^{2+}$  in square-pyramidal coordination. There is one crystallographically distinct  $M$  site occupied by Cd, Ca and  $\text{Mn}^{2+}$  coordinated by four O atoms and two (H<sub>2</sub>O) groups in a trigonal-prismatic arrangement. Variation in the occupancy of this site gives rise to the two related species andyrobetsite (Cd dominant) and calcio-andyrobetsite (Ca dominant). There is one distinct  $K$  site occupied by K and coordinated by four O atoms, two (OH) groups and two (H<sub>2</sub>O) groups in a distorted-cube arrangement. Four (CuO<sub>5</sub>) polyhedra link to a central anion to form a [Cu<sub>4</sub>O<sub>13</sub>] group. The anions at the base of this group corner-share to four (AsO<sub>4</sub>) tetrahedra that link to a fifth (CuO<sub>5</sub>) square pyramid. A single (As $\phi$ <sub>4</sub>) ( $\phi$ : unspecified anion) tetrahedron links to the central anion of the [Cu<sub>4</sub>O<sub>13</sub>] group to form a [Cu<sub>5</sub>(AsO<sub>4</sub>)<sub>4</sub>(As $\phi$ <sub>4</sub>)O<sub>9</sub>] cluster. These clusters are arranged at the vertices of non-coplanar 4<sup>4</sup> nets parallel to (100) and corner-link to form a heteropolyhedral framework with interstitial  $M$  (= Cd, Ca, Mn<sup>2+</sup>) and  $K$  (= K) sites between adjacent 4<sup>4</sup> nets. Two of the anions in the structure show anomalously low incident-bond-valence sums (1.60 and 1.69 *vu*: valence units).

*Keywords:* andyrobetsite, crystal structure, electron-microprobe analysis, arsenate, Tsumeb.

### SOMMAIRE

Nous avons résolu la structure cristalline de l'andyrobetsite, dont la composition idéale est  $K\text{Cd}[\text{Cu}^{2+}_5(\text{AsO}_4)_4\{\text{As}(\text{OH})_2\text{O}_2\}](\text{H}_2\text{O})_2$ , monoclinique,  $a$  9.8102(9),  $b$  10.0424(6),  $c$  9.9788(7) Å,  $\beta$  101.686(7)°,  $V$  962.6(1) Å<sup>3</sup>,  $P2_1/m$ ,  $Z = 2$ , par méthodes directes, et nous l'avons affinée jusqu'à un résidu  $R$  de 2.3% en utilisant 2140 réflexions observées ( $F_o > 5\sigma F$ ) mesurées avec rayonnement  $\text{MoK}\alpha$ . Il y a trois sites  $As$  cristallographiquement distincts, chacun contenant  $\text{As}^{5+}$  en coordinence tétraédrique. Un des sites  $As$  est lié à deux atomes O et deux groupes (OH) pour former un groupe arsenate doublement acide,  $\{\text{As}(\text{OH})_2\text{O}_2\}$ . Il y a quatre sites  $Cu$  cristallographiquement distincts, chacun étant occupé par  $\text{Cu}^{2+}$  en coordinence pyramidale carrée. Il y a un site  $M$  cristallographiquement distinct, dans lequel se trouvent Cd, Ca et  $\text{Mn}^{2+}$  en coordinence avec quatre atomes O et deux groupes (H<sub>2</sub>O) dans un agencement trigonal prismatique. Les variations dans ce site mènent aux deux espèces andyrobetsite (Cd dominant) et calcio-andyrobetsite (Ca dominant), présents dans le même cristal. Il y a un site distinct  $K$  occupé par K et coordonné par quatre atomes O, deux groupes (OH) et deux groupes (H<sub>2</sub>O) dans un agencement cubique difforme. Quatre polyèdres (CuO<sub>5</sub>) entourent un anion central pour former un groupe [Cu<sub>4</sub>O<sub>13</sub>]. Les anions à la base de cet agencement sont les coins de quatre tétraèdres (AsO<sub>4</sub>), qui sont connectés à une cinquième pyramide carrée (CuO<sub>5</sub>). Un seul tétraèdre (As $\phi$ <sub>4</sub>) ( $\phi$ : anion non spécifié) est lié à l'anion central du groupe [Cu<sub>4</sub>O<sub>13</sub>] pour former une agrégation de composition [Cu<sub>5</sub>(AsO<sub>4</sub>)<sub>4</sub>(As $\phi$ <sub>4</sub>)O<sub>9</sub>]. Ces agglomérations définissent les coins de réseaux 4<sup>4</sup> non coplanaires parallèles à (100), qui partagent leurs coins pour former une trame hétéropolyédrique ayant des sites interstitiels  $M$  (= Cd, Ca, Mn<sup>2+</sup>) et  $K$  (= K) entre réseaux 4<sup>4</sup> adjacents. Deux des anions dans cette structure font preuve de valences de liaison incidentes anormalement faibles (1.60 et 1.69 unités de valence).

(Traduit par la rédaction)

*Mots-clés:* andyrobetsite, structure cristalline, analyse à la microsonde électronique, arsenate, Tsumeb.

<sup>§</sup> E-mail address: frank\_hawthorne@umanitoba.ca

## INTRODUCTION

Andyrobertsite, ideally  $K Cd [Cu^{2+}_5 (AsO_4)_4 \{As(OH)_2O_2\}] (H_2O)_2$ , and calcio-andyrobertsite, ideally  $K Ca [Cu^{2+}_5 (AsO_4)_4 \{As(OH)_2O_2\}] (H_2O)_2$ , are two new minerals from Tsumeb mine, Namibia (Cooper *et al.* 1999). Both minerals form a lamellar intergrowth that is crystallographically continuous and in which the lamellae are only a few micrometers wide. However, composite crystals show high-quality diffraction patterns with small sharp diffraction-maxima, despite the composite nature of the crystals. The crystal structure of andyrobertsite – calcio-andyrobertsite was solved in order to properly characterize these minerals; the results are presented here.

## EXPERIMENTAL

Andyrobertsite – calcio-andyrobertsite from the type locality was generously made available for this work by Mr. William W. Pinch. A thin cleavage fragment ( $\parallel \{100\}$ ) was attached to a glass fiber and mounted on a Siemens P4 automated four-circle diffractometer. Cell dimensions (Table 1) were determined from the setting angles of 48 automatically aligned reflections in the range  $40 < 2\theta < 60^\circ$ . Intensities were measured from  $4$  to  $60^\circ 2\theta$  ( $\bar{1}3 \leq h \leq 13$ ,  $0 \leq k \leq 14$ ,  $0 \leq l \leq 13$ ) with scans speeds varying between  $2.0$  and  $29.3^\circ 2\theta/\text{min}$ ; a total of 3127 reflections was measured over one asymmetric unit. Psi-scan data were measured for 17 reflections uniformly distributed between  $4$  and  $60^\circ 2\theta$  at increments of psi of  $4^\circ$ . A thin-plate correction with a glancing angle of  $5^\circ$  reduced  $R(\text{azimuthal})$  from  $11.9$  to  $1.3\%$ . Intensities were corrected for Lorentz, polarization and background effects, and then reduced to structure factors; of the 2520 remaining unique reflections, 2140 were classed as observed ( $\parallel |F_o| > 5\sigma F_o$ ).

Subsequent to the diffraction experiment, the crystal used for the collection of the X-ray intensity data was analyzed with a Cameca SX-50 electron-microprobe according to the procedure described by Cooper *et al.* (1999). Back-scattered-electron (BSE) imaging of the crystal showed a fine lamellar zoning on a scale of mi-

croimeters. A traverse of 40 equidistant ( $20 \mu\text{m}$  beam size) points was acquired perpendicular to the lamellae. Each successive electron-microprobe point overlapped significantly ( $\sim 60\%$ ) with a neighboring point to provide continuous chemical sampling. The compositions of five selected points (A  $\rightarrow$  E) are given in Table 2 and shown in Figure 1 in terms of the occupancy of the  $M$  site;  $H_2O$  values were calculated from the  $H_2O$  content established by crystal-structure refinement, and unit formulae were calculated on the basis of 22 anions (including two OH and two  $H_2O$  groups). The average (bulk) composition of the crystal was estimated by weighting each of the forty compositions according to the shape of the crystal and the resulting length of the lamellae analyzed; the result is shown as + in Table 2 and Figure 1. The bulk composition of the crystal lies exactly on the boundary between andyrobertsite and calcio-andyrobertsite; for clarity of expression, we will refer to the structure as andyrobertsite.

## STRUCTURE SOLUTION AND REFINEMENT

All calculations were done with the SHELXTL PC (Plus) system of programs;  $R$  indices are of the form given in Table 1 and are expressed as percentages. The  $E$  statistics indicate a centrosymmetric structure, and the solution was found in the space group  $P2_1/m$ . All cations and anions were located by successive cycles of least-squares refinement and difference-Fourier synthesis, and refinement converged to an  $R$  index of  $2.4\%$  for a model with anisotropic-displacement parameters for all atoms (except H). Hydrogen atoms were located by bond-valence analysis and difference-Fourier synthesis,

TABLE 1. MISCELLANEOUS INFORMATION FOR ANDYROBERTSITE

|                                   |            |                          |                                 |
|-----------------------------------|------------|--------------------------|---------------------------------|
| $a$ (Å)                           | 9.8102(9)  | crystal size (mm)        | $0.015 \times 0.25 \times 0.34$ |
| $b$                               | 10.0424(6) | Radiation                | MoK $\alpha$ /Graphite          |
| $c$                               | 9.9788(7)  | Total no. of I           | 3127                            |
| $\beta$ ( $^\circ$ )              | 101.686(7) | No. of resultant I*      | 2651                            |
| $V$ (Å $^3$ )                     | 962.6(1)   | No. of $ F $             | 2520                            |
| Sp. Gr.                           | $P2_1/m$   | No. of $ F_o  > 5\sigma$ | 2140                            |
| $Z$                               | 2          | $R(\text{merge})\%$      | 1.4                             |
| $\mu\text{m}$ (mm $^{-1}$ )       | 14.95      | $R(\text{obs})\%$        | 2.3                             |
| $D_{\text{calc}}$ (g.cm $^{-3}$ ) | 4.011      | $wR(\text{obs})\%$       | 2.5                             |

\* number of I remaining after subtraction of all those intensities which had a plate-glancing angle of  $< 5^\circ$

TABLE 2. CHEMICAL COMPOSITIONS (wt.%) AND UNIT FORMULAE (apfu) OF ANDYROBERTSITE AND CALCIO-ANDYROBERTSITE FROM FIGURE 1

|                | A     | B     | C     | D     | E     | +     |
|----------------|-------|-------|-------|-------|-------|-------|
| As $_2$ O $_5$ | 47.19 | 47.87 | 48.75 | 48.97 | 49.6  | 48.35 |
| CuO            | 31.38 | 32.07 | 32.39 | 32.87 | 32.75 | 32.17 |
| ZnO            | 0.08  | 0.06  | 0.21  | 0.10  | 0.00  | 0.13  |
| CdO            | 7.12  | 5.29  | 4.09  | 2.33  | 1.30  | 4.60  |
| MnO            | 0.57  | 0.92  | 1.52  | 1.17  | 0.69  | 0.87  |
| CaO            | 1.15  | 1.58  | 1.78  | 2.86  | 3.71  | 2.01  |
| K $_2$ O       | 4.09  | 4.03  | 4.01  | 4.04  | 4.07  | 4.01  |
| (H $_2$ O)     | 4.41  | 4.47  | 4.55  | 4.57  | 4.81  | 4.51  |
| Sum            | 95.99 | 96.29 | 97.30 | 96.91 | 96.27 | 96.63 |
| As             | 5.04  | 5.04  | 5.04  | 5.03  | 5.06  | 5.05  |
| Cu             | 4.84  | 4.88  | 4.84  | 4.88  | 4.83  | 4.85  |
| Zn             | 0.01  | 0.01  | 0.03  | 0.02  | 0.00  | 0.02  |
| Cd             | 0.68  | 0.50  | 0.38  | 0.21  | 0.12  | 0.43  |
| Mn             | 0.10  | 0.16  | 0.26  | 0.20  | 0.11  | 0.15  |
| Ca             | 0.25  | 0.34  | 0.38  | 0.60  | 0.78  | 0.43  |
| K              | 1.07  | 1.04  | 1.01  | 1.01  | 1.01  | 1.02  |
| (H)            | 6     | 6     | 6     | 6     | 6     | 6     |

\* average composition along the continuous line-traverse A  $\rightarrow$  E.

and were included with constrained isotropic-displacement parameters and soft constraints on the O–H and OW–H distances ( $\approx 0.98 \text{ \AA}$ ) in the final cycles of refinement, which converged to an  $R$  index of 2.3%. Site-occupancy refinement for the cation sites shows complete chemical order over the  $As$ ,  $Cu$  and  $K$  sites, accounting for all  $As + Cu + K$  measured by chemical analysis (Table 2). The  $M$  site gives an electron sum intermediate between  $Ca$  (20 electrons) and  $Cd$  (48 electrons). The chemical analysis indicates that the remaining  $Cd + Ca + Mn$  must occur at the  $M$  site. To compare the  $Cd + Ca + Mn$  content from the unit formula (Table 2) with that from the site-occupancy refinement, the occupancy of  $Mn$  at the  $M$  site was fixed at the value from the unit formula, and the remaining scattering was then refined in terms of  $Cd$  and  $Ca$ . The occupancy of the  $M$  site refined to  $0.428(4) Ca + 0.426(4) Cd + (0.146 Mn)$ , in exact agreement with the unit formula of the crystal (Table 2). Final atom positions and displacement factors are given in Table 3, selected interatomic distances and angles for non H-atoms are listed in Table 4, interatomic distances and angles involving H atoms are given in Table 5, and a bond-valence analysis is shown in Table 6. Observed and calculated structure-factors may be obtained from The Depository of Unpublished Data, CISTI, National Research Council, Ottawa, Ontario K1A 0S2, Canada.

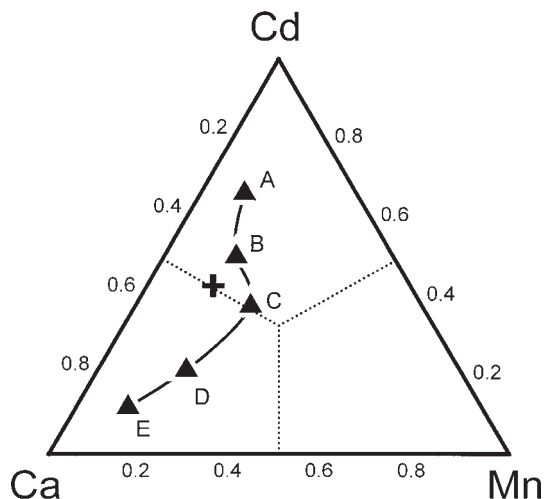


FIG. 1. Variation in chemical composition of the crystal of andyrobbersite used for crystal-structure work (marked by thick black line); the bulk composition (+) lies exactly on the boundary between andyrobbersite and calcio-andyrobbersite.

TABLE 3. ATOMIC POSITIONS AND DISPLACEMENT FACTORS\* FOR ANDYROBERTSITE

| Site  | x          | y          | z          | $U_{eq}$ | $U_{11}$ | $U_{22}$ | $U_{33}$ | $U_{23}$ | $U_{13}$ | $U_{12}$ |
|-------|------------|------------|------------|----------|----------|----------|----------|----------|----------|----------|
| As(1) | 0.18027(4) | 0.04168(4) | 0.07665(4) | 68(1)    | 80(2)    | 63(2)    | 64(2)    | -10(1)   | 20(1)    | -10(1)   |
| As(2) | 0.18285(4) | 0.04072(4) | 0.48913(4) | 77(1)    | 100(2)   | 68(2)    | 68(2)    | 5(1)     | 32(1)    | -9(1)    |
| As(3) | 0.63179(7) | 1/4        | 0.19752(7) | 166(2)   | 69(3)    | 244(3)   | 192(3)   | 0        | 39(2)    | 0        |
| Cu(1) | 0.92130(5) | 0.02668(5) | 0.23738(5) | 97(1)    | 114(2)   | 118(2)   | 65(2)    | -7(2)    | 32(2)    | -29(2)   |
| Cu(2) | 0.92830(6) | 1/4        | 0.47111(8) | 102(2)   | 127(3)   | 54(3)    | 144(3)   | 0        | 71(3)    | 0        |
| Cu(3) | 0.92803(8) | 1/4        | 0.01065(7) | 99(2)    | 113(3)   | 60(3)    | 111(3)   | 0        | -7(3)    | 0        |
| Cu(4) | 0.33062(8) | 1/4        | 0.31118(7) | 87(2)    | 124(3)   | 67(3)    | 75(3)    | 0        | 33(3)    | 0        |
| M     | 0.71729(7) | 1/4        | 0.69496(7) | 114(2)   | 102(3)   | 111(3)   | 134(3)   | 0        | 39(2)    | 0        |
| K     | 0.3562(2)  | 1/4        | 0.8281(2)  | 230(4)   | 225(7)   | 252(7)   | 237(7)   | 0        | 106(6)   | 0        |
| O(1)  | 0.1756(4)  | 0.0779(3)  | 0.9134(3)  | 152(9)   | 217(16)  | 156(14)  | 93(12)   | -20(11)  | 55(12)   | -101(13) |
| O(2)  | 0.8212(3)  | 0.1228(3)  | 0.8847(3)  | 128(8)   | 174(15)  | 58(12)   | 135(13)  | 20(11)   | -13(12)  | 1(11)    |
| O(3)  | 0.3242(3)  | 0.1082(3)  | 0.1724(3)  | 126(8)   | 96(13)   | 138(13)  | 136(13)  | -69(11)  | 5(11)    | -10(12)  |
| O(4)  | 0.0358(3)  | 0.1107(3)  | 0.1204(3)  | 103(6)   | 98(13)   | 113(13)  | 109(12)  | 22(10)   | 44(11)   | 27(11)   |
| O(5)  | 0.8297(3)  | 0.1207(3)  | 0.5618(3)  | 118(8)   | 153(14)  | 62(12)   | 157(14)  | -17(11)  | 78(12)   | -13(11)  |
| O(6)  | 0.0342(3)  | 0.1120(3)  | 0.4008(3)  | 104(6)   | 114(13)  | 107(13)  | 92(12)   | -11(10)  | 23(11)   | 19(11)   |
| O(7)  | 0.3232(3)  | 0.1101(3)  | 0.4471(3)  | 134(8)   | 126(14)  | 141(13)  | 140(13)  | 43(11)   | 35(12)   | -19(12)  |
| O(8)  | 0.1934(4)  | 0.0630(3)  | 0.6562(3)  | 165(9)   | 205(15)  | 230(15)  | 68(12)   | -6(12)   | 47(11)   | -100(14) |
| O(9)  | 0.8050(5)  | 1/4        | 0.2178(6)  | 206(14)  | 73(20)   | 240(23)  | 300(26)  | 0        | 25(19)   | 0        |
| O(10) | 0.5653(5)  | 1/4        | 0.3363(5)  | 234(15)  | 129(22)  | 382(29)  | 191(23)  | 0        | 35(19)   | 0        |
| OH    | 0.5733(5)  | 0.1154(5)  | 0.0936(5)  | 423(15)  | 252(20)  | 627(30)  | 438(24)  | -277(23) | 182(19)  | -252(22) |
| OW    | 0.5326(4)  | 0.1078(3)  | 0.6744(4)  | 202(10)  | 161(15)  | 158(14)  | 275(17)  | -3(14)   | 18(14)   | 15(13)   |
| H(1)  | 0.465(5)   | 0.111(6)   | 0.587(3)   | 200**    |          |          |          |          |          |          |
| H(2)  | 0.594(5)   | 0.034(4)   | 0.662(6)   | 200**    |          |          |          |          |          |          |
| H(3)  | 0.479(2)   | 0.097(6)   | 0.106(6)   | 200**    |          |          |          |          |          |          |

\*  $U = \exp[-2\pi^2(h^2a^2U_{11} + k^2b^2U_{22} + l^2c^2U_{33} + 2hkaU_{12} + 2hlaU_{13} + 2klcU_{23})] \times 10^4 \text{ \AA}^2$ .

\*\* constrained during refinement.

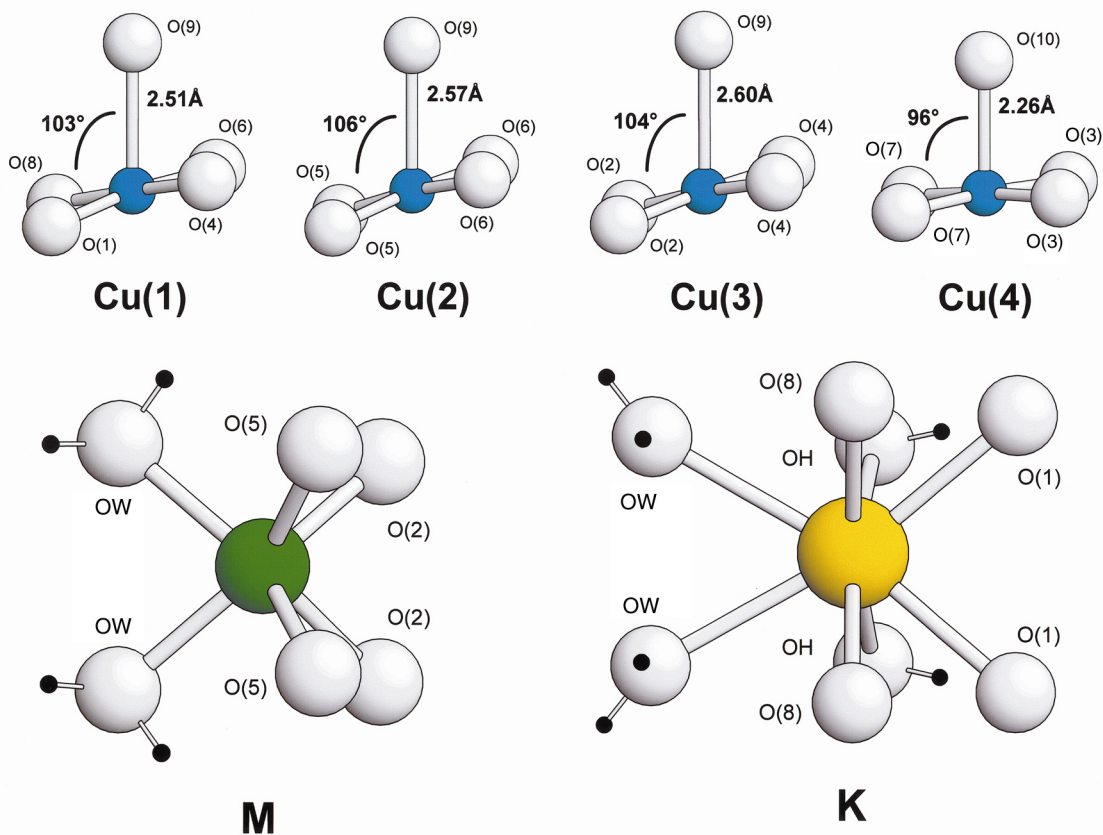


FIG. 2. Cation coordination in andyrobbersite; blue circles:  $\text{Cu}^{2+}$  atoms; grey highlighted circles: O atoms; small black circles: H atoms; large green circle: *M*-site atom; large yellow highlighted circle: K atom.

## DESCRIPTION OF THE STRUCTURE

### Coordination of the cations

There are three crystallographically distinct *As* sites, each occupied by  $\text{As}^{5+}$  coordinated by four O atoms in a tetrahedral arrangement. The relative dispersion of the bond lengths in each tetrahedron is not large; despite their unusual connectivity, the  $\text{As}(3)\phi_4$  tetrahedron is somewhat more distorted than the  $\text{As}(1)\text{O}_4$  and  $\text{As}(2)\text{O}_4$  tetrahedra, but none of the distortions are particularly large. As the bond topology of this structure is rather unusual, we also list the  $\phi-\phi$  and  $\phi-\text{As}-\phi$  angles in Table 4.

There are four crystallographically distinct *Cu* sites, each occupied by  $\text{Cu}^{2+}$  coordinated by five O atoms in distorted square-pyramidal arrangements (Fig. 2). In all cases, the four meridional  $\text{Cu}^{2+}-\text{O}$  bonds are short (1.92–1.98 Å), and the apical bond is long (2.27–2.60 Å). The deviation from equal bond-lengths in the ( $\text{CuO}_5$ ) polyhedra is much larger than is normal in such

polyhedra in minerals (Eby & Hawthorne 1990, Burns & Hawthorne 1995). The square-pyramidal geometries of the ( $\text{CuO}_5$ ) polyhedra show significant bond-elongation to the apical oxygen [O(9)], in addition to large angular deviations between the apical and equatorial oxygen atoms (Fig. 2). The geometry for  $\text{Cu}(4)\text{O}_5$  shows only marginal deviation from that normally observed for  $\text{Cu}^{2+}$  in square-pyramidal coordination. It should be noted that this distortion does not seem to be induced by the bond-valence requirements at the O(9) and O(10) sites (those sites involved in the apical bonds) as the anions at these sites show anomalously low incident bond-valence sums (Table 6).

There is one crystallographically distinct *M* site that is occupied by Cd, Ca and  $\text{Mn}^{2+}$ . Indeed, the chemical composition of the crystal used to collect the X-ray intensity data (Fig. 1) indicates that both the Cd and Ca species (andyrobbersite and calcio-andyrobbersite, respectively) are present in the crystal, and in places, the composition approaches fairly closely to the (as yet not found)  $\text{Mn}^{2+}$ -dominant species. The *M* site is surrounded

by four O atoms and two (H<sub>2</sub>O) groups in a trigonal-prismatic arrangement (Fig. 2), and the dispersion of the  $M-\phi$  ( $\phi = \text{O}^{2-}, \text{H}_2\text{O}$ ) bonds is fairly small (Table 4).

There is one crystallographically distinct  $K$  site, occupied by  $K$  and coordinated by four O atoms, two (OH) groups and two (H<sub>2</sub>O) groups in a distorted-cube arrangement (Fig. 2), with significant dispersion (2.73–3.33 Å) in the individual  $K-\phi$  bond-lengths.

### STRUCTURE TOPOLOGY

The key element of the andyrobertsite structure is a [Cu<sub>5</sub> (AsO<sub>4</sub>)<sub>4</sub> (Asφ<sub>4</sub>) O<sub>9</sub>] cluster that is illustrated by ball-and-stick and polyhedral diagrams in Figure 3. Four (CuO<sub>5</sub>) groups [involving two  $Cu(1)$ , one  $Cu(2)$  and one  $Cu(3)$  sites] link to a central O(9) anion, sharing edges

to form a [Cu<sub>4</sub>O<sub>13</sub>] group (Figs. 3a, b). The base of this group is decorated by four (AsO<sub>4</sub>) tetrahedra [involving two  $As(1)$  and two  $As(2)$  sites] that corner-share to the four basal oxygen atoms of the  $Cu(4)$ O<sub>5</sub> square pyramid. A single (Asφ<sub>4</sub>) tetrahedron attaches to the central O(9) anion of the [Cu<sub>4</sub>O<sub>13</sub>] group to form the complete [Cu<sub>5</sub> (AsO<sub>4</sub>)<sub>4</sub> (Asφ<sub>4</sub>) O<sub>9</sub>] cluster (Figs. 3c, d).

These clusters are arranged at the vertices of a slightly corrugated 4<sup>4</sup> net parallel to (100) to form a sheet (Fig. 4). Adjacent clusters are displaced from each other by ( $b/2 + c/2$ ), and adjacent [Cu<sub>5</sub> (AsO<sub>4</sub>)<sub>4</sub> (Asφ<sub>4</sub>) O<sub>9</sub>] clusters are inverted in the [100] direction (Fig. 4). Clusters link directly by sharing peripheral vertices of the outer arsenate groups of one cluster with meridional anions of (CuO<sub>5</sub>) polyhedra in adjacent clusters (Fig. 4). The result is a thick slab that resembles a chess board with one color occupied by [Cu<sub>5</sub> (AsO<sub>4</sub>)<sub>4</sub> (Asφ<sub>4</sub>) O<sub>9</sub>] clusters.

The stacking of these slabs is shown in Figure 5. The slabs are linked by sharing of apical  $Cu(4)$ O<sub>5</sub> vertices

TABLE 4. SELECTED INTERATOMIC DISTANCES (Å) AND ANGLES (°) FOR ANDYROBERTSITE

|                      |                    |                   |                 |  |  |
|----------------------|--------------------|-------------------|-----------------|--|--|
| As(1)–O(1)a          | 1.661(3)           | Cu(1)–O(1)b       | 1.921(3)        |  |  |
| As(1)–O(2)b          | 1.697(3)           | Cu(1)–O(4)e       | 1.967(3)        |  |  |
| As(1)–O(3)           | 1.675(3)           | Cu(1)–O(6)e       | 1.972(3)        |  |  |
| As(1)–O(4)           | <u>1.712(3)</u>    | Cu(1)–O(8)b       | 1.921(4)        |  |  |
| <As(1)–O>            | 1.686              | Cu(1)–O(9)        | <u>2.506(2)</u> |  |  |
|                      |                    | <Cu(1)–O>         | 2.057           |  |  |
| As(2)–O(5)b          | 1.695(3)           |                   |                 |  |  |
| As(2)–O(6)           | 1.702(3)           | Cu(2)–O(5)        | 1.949(3) x2     |  |  |
| As(2)–O(7)           | 1.670(3)           | Cu(2)–O(6)e,f     | 1.946(3) x2     |  |  |
| As(2)–O(8)           | <u>1.664(3)</u>    | Cu(2)–O(9)        | <u>2.572(5)</u> |  |  |
| <As(2)–O>            | 1.683              | <Cu(2)–O>         | 2.072           |  |  |
| As(3)–O(9)           | 1.670(5)           | Cu(3)–O(2)a,d     | 1.944(3) x2     |  |  |
| As(3)–O(10)          | 1.646(6)           | Cu(3)–O(4)e,f     | 1.950(3) x2     |  |  |
| As(3)–OH,c           | <u>1.730(5)</u> x2 | Cu(3)–O(9)        | <u>2.597(6)</u> |  |  |
| <As(3)–O>            | 1.694              | <Cu(3)–O>         | 2.077           |  |  |
| K–O(1),c             | 2.731(4) x2        | Cu(4)–O(3),c      | 1.978(3) x2     |  |  |
| K–O(8),c             | 2.812(3) x2        | Cu(4)–O(7),c      | 1.965(3) x2     |  |  |
| K–OHg,h              | 3.331(5) x2        | Cu(4)–O(10)       | <u>2.265(5)</u> |  |  |
| K–OW                 | <u>2.909(4)</u> x2 | <Cu(4)–O>         | 2.030           |  |  |
| <K–O>                | 2.946              |                   |                 |  |  |
| M–O(2),c             | 2.339(3) x2        |                   |                 |  |  |
| M–O(5),c             | 2.294(3) x2        |                   |                 |  |  |
| M–OW,c               | <u>2.283(4)</u> x2 |                   |                 |  |  |
| <M–O>                | 2.305              |                   |                 |  |  |
| As(1) tetrahedron    |                    |                   |                 |  |  |
| O(1)a–O(2)b          | 2.846(4)           | O(1)a–As(1)–O(2)b | 115.9(2)        |  |  |
| O(1)a–O(3)           | 2.715(4)           | O(1)a–As(1)–O(3)  | 108.9(2)        |  |  |
| O(1)a–O(4)           | 2.721(5)           | O(1)a–As(1)–O(4)  | 107.6(2)        |  |  |
| O(2)b–O(3)           | 2.722(4)           | O(2)b–As(1)–O(3)  | 107.7(1)        |  |  |
| O(3)–O(4)            | 2.771(4)           | O(3)–As(1)–O(4)   | 109.8(1)        |  |  |
| O(4)–O(2)b           | <u>2.738(4)</u>    | O(4)–As(1)–O(2)b  | <u>106.9(2)</u> |  |  |
| <O–O>                | 2.752              | <O–As(1)–O>       | 109.5           |  |  |
| As(2) tetrahedron    |                    |                   |                 |  |  |
| O(5)b–O(6)           | 2.679(4)           | O(5)b–As(2)–O(6)  | 104.1(1)        |  |  |
| O(5)b–O(7)           | 2.752(4)           | O(5)b–As(2)–O(7)  | 109.7(2)        |  |  |
| O(5)b–O(8)           | 2.826(4)           | O(5)b–As(2)–O(8)  | 114.5(2)        |  |  |
| O(6)–O(7)            | 2.778(4)           | O(6)–As(2)–O(7)   | 111.0(1)        |  |  |
| O(7)–O(8)            | 2.696(5)           | O(7)–As(2)–O(8)   | 107.9(2)        |  |  |
| O(8)–O(6)            | <u>2.750(4)</u>    | O(8)–As(2)–O(6)   | <u>109.6(2)</u> |  |  |
| <O–O>                | 2.747              | <O–As(2)–O>       | 109.5           |  |  |
| As(3) tetrahedron    |                    |                   |                 |  |  |
| O(9)–O(10)           | 2.837(8)           | O(9)–As(3)–O(10)  | 117.7(3)        |  |  |
| O(9)–OH              | 2.718(6) x2        | O(9)–As(3)–OH     | 106.2(2)        |  |  |
| O(10)–OH             | 2.789(7) x2        | O(10)–As(3)–OH    | 111.4(2)        |  |  |
| OH–OHc               | <u>2.704(11)</u>   | OH–As(3)–OHc      | <u>102.8(3)</u> |  |  |
| <O–O>                | 2.759              | <O–As(3)–O>       | 109.3           |  |  |
| Cu(1) square pyramid |                    |                   |                 |  |  |
| O(9)–O(1)b           | 3.563(4)           | O(9)–Cu(1)–O(1)b  | 106.4(1)        |  |  |
| O(9)–O(4)e           | 2.987(6)           | O(9)–Cu(1)–O(4)e  | 82.9(2)         |  |  |
| O(9)–O(6)e           | 2.941(5)           | O(9)–Cu(1)–O(6)e  | 81.1(1)         |  |  |
| O(9)–O(8)b           | 3.385(4)           | O(9)–Cu(1)–O(8)b  | 98.9(2)         |  |  |
| O(1)b–O(4)e          | 2.778(4)           | O(1)b–Cu(1)–O(4)e | 91.2(1)         |  |  |
| O(4)e–O(6)e          | 2.801(4)           | O(4)e–Cu(1)–O(6)e | 90.7(1)         |  |  |
| O(6)e–O(8)b          | 2.808(5)           | O(6)e–Cu(1)–O(8)b | 92.3(1)         |  |  |
| O(8)b–O(1)b          | <u>2.612(4)</u>    | O(8)b–Cu(1)–O(1)b | <u>85.7(1)</u>  |  |  |
| <O–O>                | 2.984              | <O–Cu(1)–O>       | 91.2            |  |  |
| Cu(2) square pyramid |                    |                   |                 |  |  |
| O(9)–O(5)            | 3.632(6) x2        | O(9)–Cu(2)–O(5)   | 106.1(1)        |  |  |
| O(9)–O(6)e           | 2.941(5) x2        | O(9)–Cu(2)–O(6)e  | 79.9(1)         |  |  |
| O(5)–O(6)e           | 2.815(5) x2        | O(5)–Cu(2)–O(6)e  | 92.6(1)         |  |  |
| O(6)e–O(6)f          | 2.771(6)           | O(6)e–Cu(2)–O(6)f | 90.8(2)         |  |  |
| O(5)c–O(5)           | <u>2.598(6)</u>    | O(5)c–Cu(2)–O(5)  | <u>83.6(2)</u>  |  |  |
| <O–O>                | 3.018              | <O–Cu(2)–O>       | 91.5            |  |  |
| Cu(3) square pyramid |                    |                   |                 |  |  |
| O(9)–O(2)a           | 3.595(6) x2        | O(9)–Cu(3)–O(2)a  | 103.8(1)        |  |  |
| O(9)–O(4)e           | 2.987(6) x2        | O(9)–Cu(3)–O(4)e  | 80.8(1)         |  |  |
| O(2)a–O(4)e          | 2.824(4) x2        | O(2)a–Cu(3)–O(4)e | 93.0(1)         |  |  |
| O(4)e–O(4)f          | 2.797(6)           | O(4)e–Cu(3)–O(4)f | 91.6(2)         |  |  |
| O(2)d–O(2)a          | <u>2.555(6)</u>    | O(2)d–Cu(3)–O(2)a | <u>82.2(2)</u>  |  |  |
| <O–O>                | 3.021              | <O–Cu(3)–O>       | 91.1            |  |  |
| Cu(4) square pyramid |                    |                   |                 |  |  |
| O(10)–O(3)           | 2.955(5) x2        | O(10)–Cu(4)–O(3)  | 88.0(1)         |  |  |
| O(10)–O(7)           | 3.147(6) x2        | O(10)–Cu(4)–O(7)  | 95.9(1)         |  |  |
| O(3)–O(7)            | 2.744(4) x2        | O(3)–Cu(4)–O(7)   | 88.2(1)         |  |  |
| O(7)–O(7)c           | 2.810(6)           | O(7)–Cu(4)–O(7)c  | 91.3(2)         |  |  |
| O(3)–O(3)c           | <u>2.847(6)</u>    | O(3)–Cu(4)–O(3)c  | <u>92.0(2)</u>  |  |  |
| <O–O>                | 2.919              | <O–Cu(4)–O>       | 90.9            |  |  |

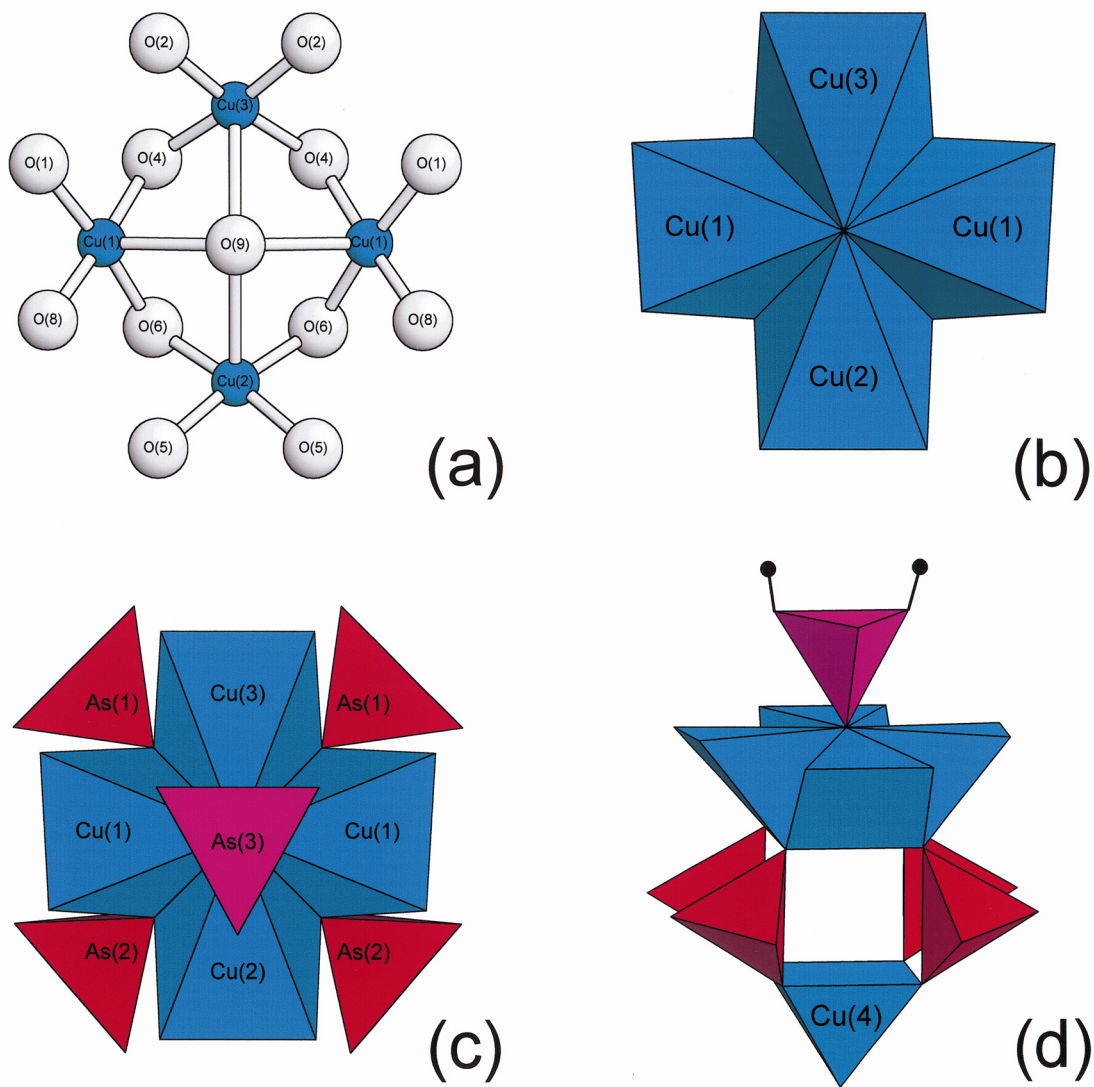


FIG. 3. The stereochemistry of the  $[\text{Cu}_5(\text{AsO}_4)_4(\text{As}\phi_4)\text{O}_9]$  cluster in andyrobertsite; (a) ball-and-stick model of the  $[\text{Cu}_4\text{O}_{13}]$  group, legend as in Figure 2, (b) polyhedral model of the  $[\text{Cu}_4\text{O}_{13}]$  group viewed down  $[100]$ ; (CuO<sub>5</sub>) polyhedra are blue; (c), (d) polyhedral model of the  $[\text{Cu}_5(\text{AsO}_4)_4(\text{As}\phi_4)\text{O}_9]$  cluster viewed down  $[100]$  and perspective view, respectively; legend as in Figure 3(b) with the  $\text{As}\phi_4$  tetrahedra shown in pink.

with O vertices of the  $\text{As}(3)\phi_4$  tetrahedra to form a continuous  $\text{Cu}\phi_5\text{-As}\phi_4$  framework. Further interslab linkage is provided by H-bonding between the (OH) groups of the doubly acid arsenate tetrahedron and two meridional O atoms of the  $\text{Cu}(4)\text{O}_5$  polyhedron.

In the view of the structure shown in Figure 4, andyrobertsite appears orthorhombic; Figure 5 shows why the structure is actually monoclinic. The  $\text{Cu}(4)\text{O}_5$  polyhedron links clusters adjacent in the  $a$  direction via the  $\text{Cu}(4)\text{-O}$  apical bond. This bond is coaxial with the

central axis of one cluster, but links to the basal O atom of the  $\text{As}(3)\phi_4$  tetrahedron; as the latter anion is off the central axis of the adjacent cluster, adjacent clusters are systematically offset along  $-c$  as they link along  $a$  (Fig. 5).

The overall structure is a highly complicated framework of  $\text{As}\phi_4$  tetrahedra and  $(\text{CuO}_5)$  square pyramids, with Cd, K and  $\text{H}_2\text{O}$  occupying the interstices and strengthening the framework (Fig. 6). Above, it was noted that the  $[\text{Cu}_5(\text{AsO}_4)_2(\text{As}\phi_4)\text{O}_9]$  clusters occupy

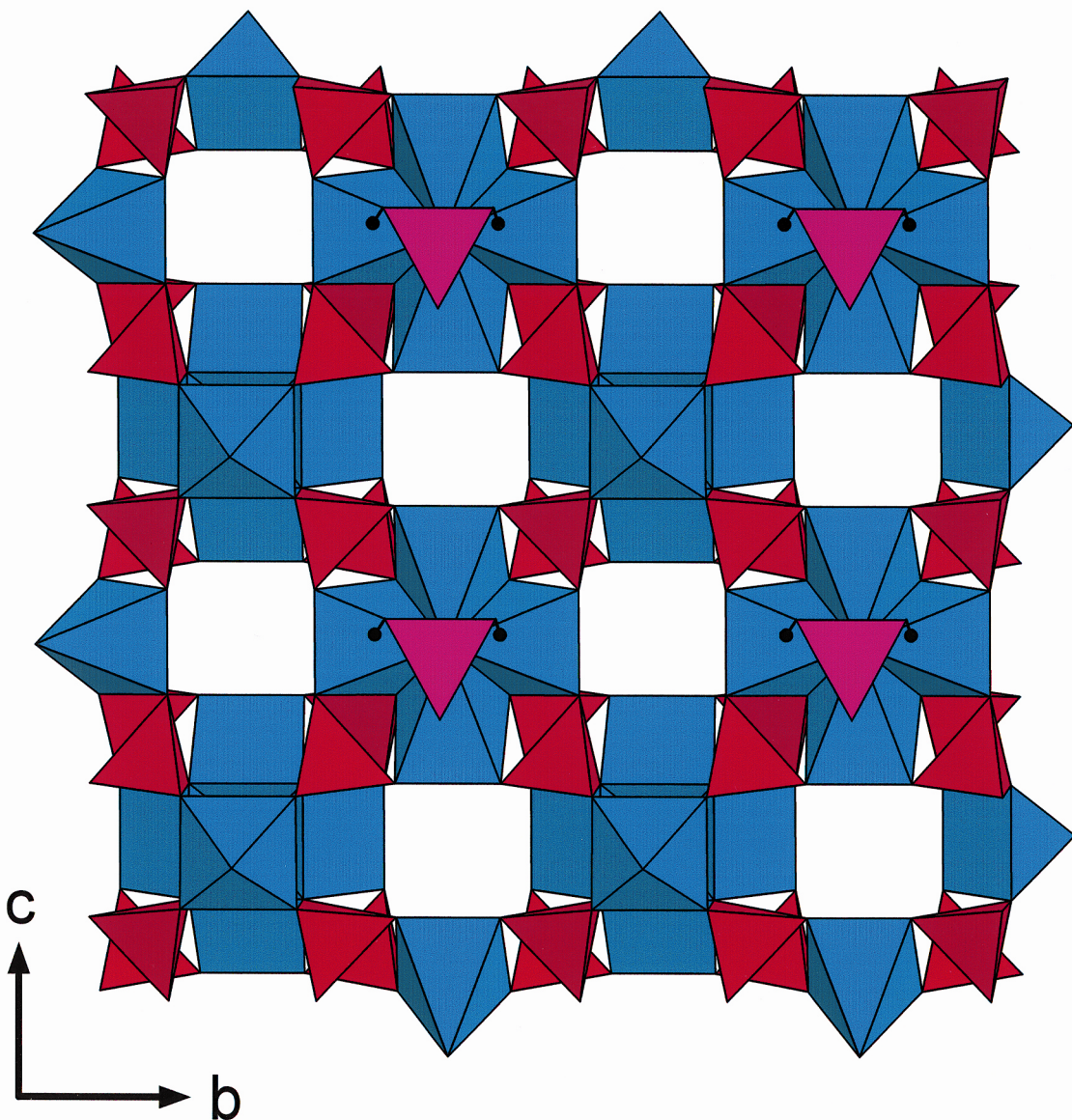


FIG. 4. The heteropolyhedral  $(\text{CuO}_5)\text{--}(\text{As}\phi_4)$  slab in andyrobbersite, projected down an axis  $6^\circ$  from  $[100]$ ; legend as in Figure 3.

alternate vertices of a  $4^4$  net. In Figure 6, it can be seen that the other set of alternate vertices is occupied by the  $M$  and  $K$  sites. In Figure 6, only the  $M$  and  $K$  sites proximal to the upper surface of the slab are seen. Attached to the lower surface (not shown) is an  $M$  site beneath every  $K$  site, and a  $K$  site beneath every  $M$  site. Linkage between adjacent slabs occurs *via* (1) the shared  $\text{H}_2\text{O}\text{--}\text{H}_2\text{O}$  edge between adjacent  $M\phi_6$  and  $K\phi_8$  polyhedra and

(2) the shared  $\text{OH}\text{--}\text{OH}$  edge between adjacent  $\text{As}(3)\phi_4$  and  $K\phi_8$  polyhedra.

#### Hydrogen bonding

The bond-valence analysis (Table 6) indicates that there is one (OH) group and one ( $\text{H}_2\text{O}$ ) group in the andyrobbersite structure; details of their stereochemis-

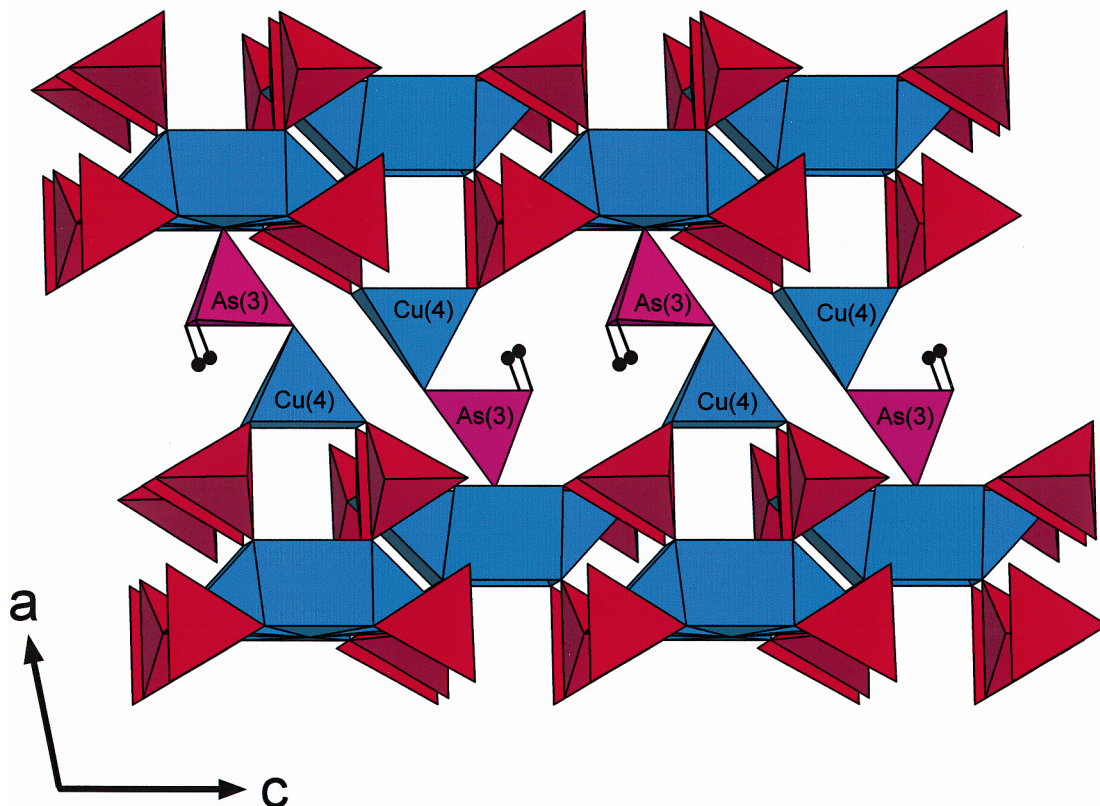


Fig. 5. The  $(\text{CuO}_3)\text{--}(\text{As}\phi_4)$  framework in andyrobertsite projected down an axis  $6^\circ$  from  $[010]$ ; legend as in Figure 3.

try (Table 5) lie in the ranges typical for H-bonding (Ferraris & Franchini-Angela 1972, Chiari & Ferraris 1982, Ferraris & Ivaldi 1984) and are illustrated in Figure 7.

The (OH) group is bonded to As at the  $\text{As}(3)$  site to form a doubly acid arsenate group:  $\{\text{As}(\text{OH})_2\text{O}_2\}$ . This is the third example of a doubly acid arsenate group to

be found in a mineral. Kaatialaite,  $\text{Fe}^{3+}\{\text{As}(\text{OH})_2\text{O}_2\}_3(\text{H}_2\text{O})_{5.5}$  (Boudjada & Guitel 1981, Schmetzer & Medenbach 1986), and the unnamed phase  $\text{Ca}\{\text{As}(\text{OH})_2\text{O}_2\}_2$  described by Ondruš *et al.* (1997) each contain an  $\{\text{As}(\text{OH})_2\text{O}_2\}$  group.

Ferraris & Ivaldi (1984) examined the stereochemistry of protonated arsenates and showed that there are strong correlations between the  $\text{As}\text{--}\text{OH}$  and  $\text{O}\text{--}\text{H}$  distances and between the  $\text{As}\text{--}(\text{OH})$  and  $\text{H}\dots\text{O}$  distances; despite the fact that soft constraints on the H-atom positions were used in the refinement of the structure of andyrobertsite, the stereochemical data for andyrobertsite are in almost exact accord with the  $\text{As}\text{--}\text{OH}$  versus  $\text{H}\dots\text{O}$  trend of Ferraris & Ivaldi (1984): in andyrobertsite, the H atom at H(3) H-bonds to the O(3) atom of the adjacent  $\text{Cu}(4)\text{O}_5$  polyhedron (Fig. 7a). The  $\text{Cu}(4)\text{O}_5$  polyhedron also links directly to the  $\text{As}(3)\phi_4$  tetrahedron through the O(10) atom.

The  $(\text{H}_2\text{O})$  group links directly to the  $M$ -site cation (Fig. 7b), and hence must H-bond to adjacent anions to satisfy its own bond-valence requirements. There is a single H-bond by the H atom at H(1) to an O(7) anion

TABLE 5. DETAILS OF H-BONDING IN ANDYROBERTSITE

|          |           |                 |           |
|----------|-----------|-----------------|-----------|
| OH-H(3)  | 0.98(3) Å | H(3).....O(3)   | 1.77(4) Å |
| OH-O(3)  | 2.716(6)  | OH-H(3)---O(3)  | 160(6) °  |
| OW-H(1)  | 0.98(3)   | H(1).....O(7)   | 1.76(3) Å |
| OW-H(2)  | 0.98(5)   | H(2).....O(3)b  | 2.21(5)   |
|          |           | H(2).....O(7)b  | 2.07(5)   |
| OW-O(7)  | 2.735(4)  | OW-H(1)---O(7)  | 170(4) °  |
| OW-O(3)b | 2.854(4)  | OW-H(2)---O(3)b | 123(4)    |
| OW-O(7)b | 2.992(5)  | OW-H(2)---O(7)b | 155(4)    |

Symmetry operators: a:  $x, y, z-1$ ; b:  $\bar{x}+1, \bar{y}, \bar{z}+1$ ; c:  $x, \bar{y}+1/2, z$ ; d:  $x, \bar{y}+1/2, z-1$ ; e:  $x+1, y, z$ ; f:  $x+1, \bar{y}+1/2, z$ ; g:  $x, y, z+1$ ; h:  $x, \bar{y}+1/2, z+1$

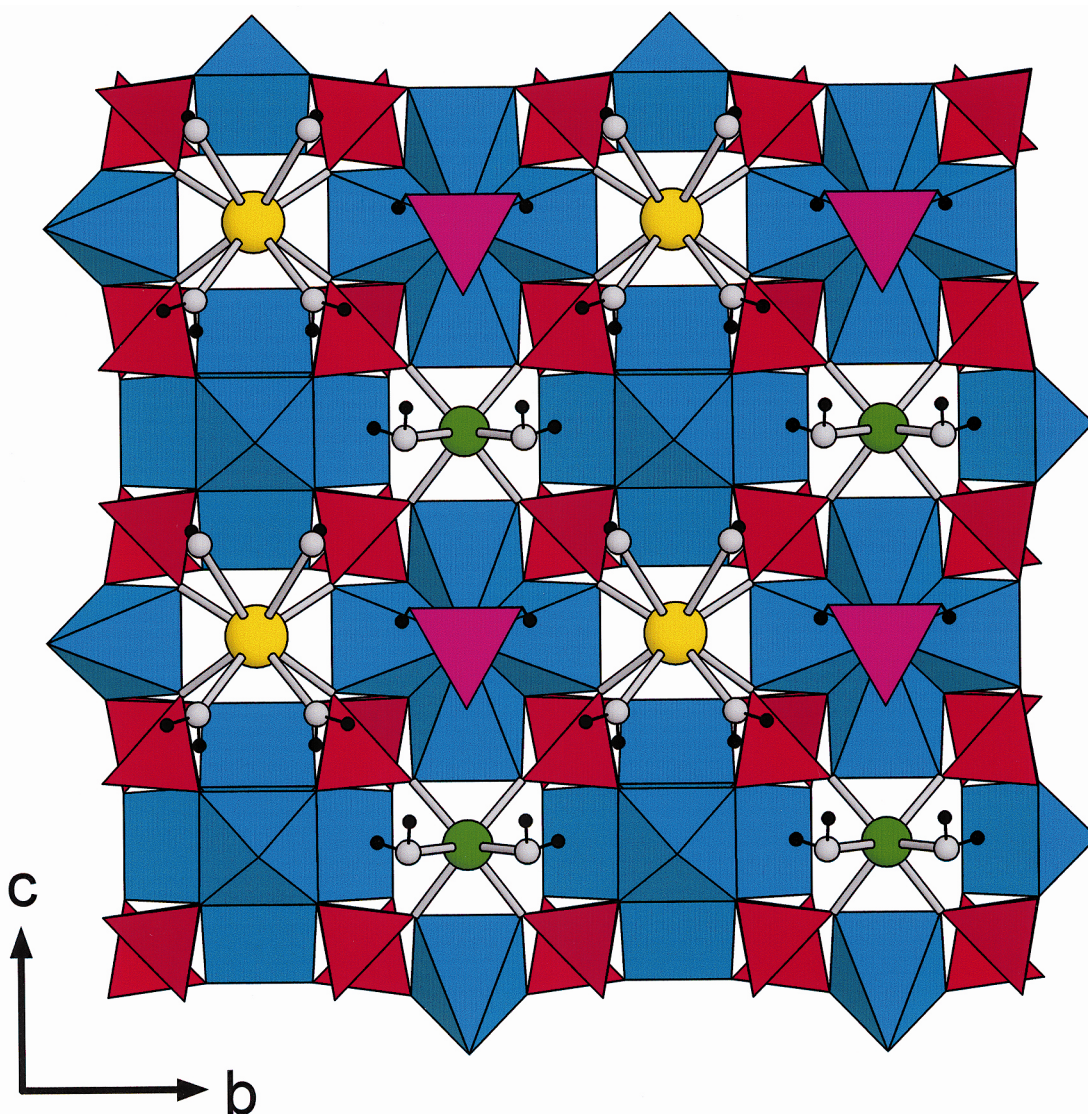


FIG. 6. The structure of andyrobetsite projected onto (100); legend as in Figures 2 and 3.

of an adjacent  $As(2)O_4$  group, and a bifurcated H-bond by the H atom at H(2) to adjacent O(3) and O(7) anions (Fig. 7b). The resulting bond-valence sums at the O(3) and O(7) anions are close to the ideal value of  $2 \text{ vu}$  (Table 6).

#### HIGHLY UNDERSATURATED ANIONS IN THE ANDYROBERTSITE STRUCTURE

Inspection of Table 6 shows that all cations have bond-valence sums near their ideal expected values, and

that the magnitude of the grand sum for all bonds ( $44.25 \text{ vu}$ ) is very near the ideal total ( $44 \text{ vu}$ ) *pfu*. Most valence sums at the anions are near their expected ideal value ( $2 \text{ vu}$ ); however, sums at O(9) and O(10) are anomalously low at 1.69 and 1.60 *vu*, respectively. Valence sums calculated for well-refined structures normally fall within 10% of their ideal value, whereas the valence sums at O(9) and O(10) are low by 15 and 20%, respectively. Bonding in this region of the structure thus needs to be examined further. The O(9) and O(10) sites occur on a mirror plane, whereas all other anions occur at gen-

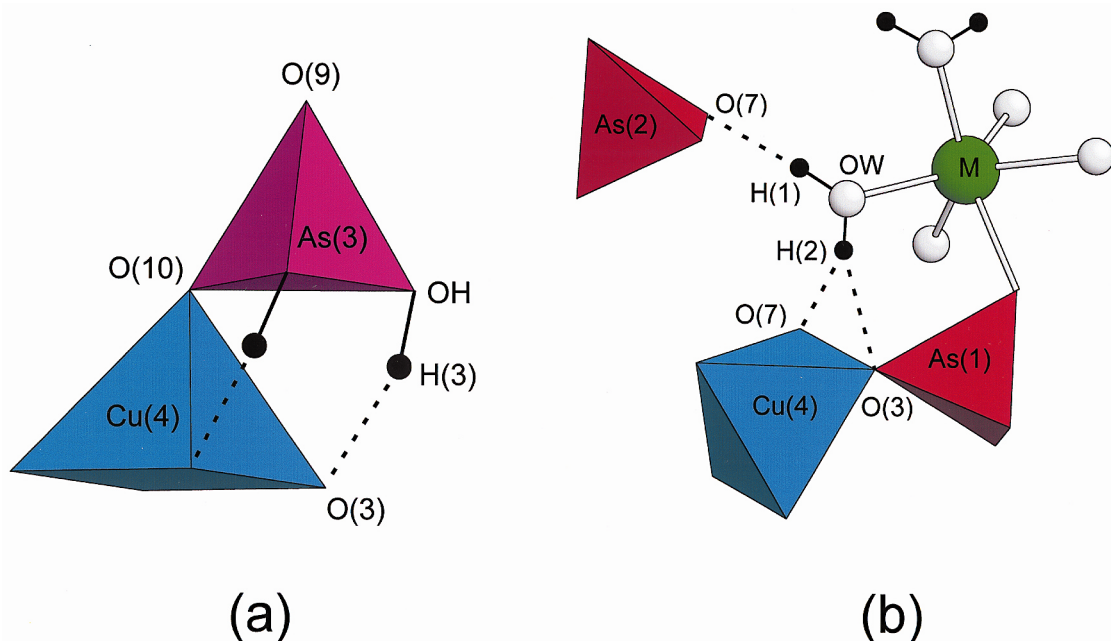


FIG. 7. Perspective views of the H-bond arrangement in andyrobbersite: (a) the (OH) group; (b) the (H<sub>2</sub>O) group, designated OW; proposed H-bonds are shown as broken lines.

eral positions; thus, on a *pfu* basis, the small bond-valence excesses ( $> 2 \text{ vu}$ ) at several of the anions more than offset the large bond-valence deficits at O(9) and O(10). The bond-valence sums in Table 6 indicate the following with respect to bonding in the andyrobbersite structure: (1) anomalously low bond-valence sums at O(9) and O(10), (2) compensatory small excesses of bond-valence at the other anion sites, and (3) normal bond-valence sums at all cation sites.

#### The local environments of O(9) and O(10)

The O(9) anion is bonded to four Cu<sup>2+</sup> cations [Cu(1)  $\times$  2, Cu(2), Cu(3)] and one As<sup>5+</sup> cation [As(3)] with bond-valence contributions of  $4 \times \sim 0.10$  and 1.30 *vu*, respectively. The O(9) anion occurs at the core of the [Cu<sub>5</sub>(AsO<sub>4</sub>)<sub>4</sub>(As $\phi$ )<sub>4</sub>O<sub>9</sub>] cluster (Fig. 3). No other cations (including H) are sufficiently close to bond to O(9); moreover, the neighborhood of O(9) is too spatially constricted to accommodate another cation.

The O(10) anion is bonded to one As<sup>5+</sup> cation [As(3)] and one Cu<sup>2+</sup> cation [Cu(4)], with bond-valence contributions of 1.39 and 0.21 *vu*, respectively (Figs. 5, 7). No additional cations (including H) are sufficiently close to bond to O(10), although there is considerable space around O(10) in the structure. We conclude that the bond-valence deficiencies at O(9) and O(10) do not result from unrecognized chemical bonds in the struc-

ture. The O(9) and O(10) anions form an edge of the As(3) $\phi$ <sub>4</sub> tetrahedron, and the individual As(3)– $\phi$  bonds and  $\phi$ –As(3)– $\phi$  angles are in the usual range (Table 4). However, the connectivity of the As(3) $\phi$ <sub>4</sub> tetrahedron in the andyrobbersite structure is very unusual; one vertex [O(9)] of the As(3) $\phi$ <sub>4</sub> tetrahedron is coordinated by five cations, another vertex [O(10)] is coordinated by two cations, and the remaining vertices are [1]-coordinated OH groups. As a result, there is no single strong bond ( $> 0.2 \text{ vu}$ ) that forms between any of the vertices of the As(3) $\phi$ <sub>4</sub> tetrahedron and the neighboring cations (Table 6).

#### Anisotropic displacements in the andyrobbersite structure

A cursory glance at Table 3 shows rather prominent anisotropy at many of the sites. Without going into minutiae, we can summarize the observed isotropy–anisotropy relations in the following manner: at the core of the [Cu<sub>5</sub>(AsO<sub>4</sub>)<sub>4</sub>(As $\phi$ )<sub>4</sub>O<sub>9</sub>] cluster is a rigid cube of atoms defined by isotropic anions O(4), O(6), O(3) and O(7) at its eight corners. Joined to the top surface of this cube along each of the four edges are four distorted (CuO<sub>5</sub>) polyhedra. Each (CuO<sub>5</sub>) of the [Cu<sub>4</sub>O<sub>13</sub>] group is securely anchored at its base but has the freedom to bend and flex. The loosely attached As(3) $\phi$ <sub>4</sub> tetrahedron sits atop the [Cu<sub>4</sub>O<sub>13</sub>] group, exhibiting lateral displace-

TABLE 6. BOND-VALENCE\* ( $\nu u$ ) TABLE FOR ANDYROBERTSITE

|          | As(1) | As(2) | As(3)               | Cu(1)               | Cu(2)               | Cu(3)               | Cu(4)               | M                   | K                   | H(1) | H(2) | H(3) | $\Sigma$ |
|----------|-------|-------|---------------------|---------------------|---------------------|---------------------|---------------------|---------------------|---------------------|------|------|------|----------|
| O(1)     | 1.33  |       |                     | 0.52                |                     |                     |                     |                     | 0.20 <sup>2</sup> ↓ |      |      |      | 2.05     |
| O(2)     | 1.21  |       |                     |                     |                     | 0.49 <sup>2</sup> ↓ |                     | 0.32 <sup>2</sup> ↓ |                     |      |      |      | 2.02     |
| O(3)     | 1.28  |       |                     |                     |                     |                     | 0.45 <sup>2</sup> ↓ |                     |                     | 0.08 | 0.20 |      | 2.01     |
| O(4)     | 1.16  |       |                     | 0.46                |                     | 0.48 <sup>2</sup> ↓ |                     |                     |                     |      |      |      | 2.10     |
| O(5)     |       | 1.21  |                     |                     | 0.48 <sup>2</sup> ↓ |                     |                     | 0.36 <sup>2</sup> ↓ |                     |      |      |      | 2.05     |
| O(6)     |       | 1.19  |                     | 0.45                | 0.49 <sup>2</sup> ↓ |                     |                     |                     |                     |      |      |      | 2.13     |
| O(7)     |       | 1.30  |                     |                     |                     |                     | 0.46 <sup>2</sup> ↓ |                     |                     | 0.20 | 0.08 |      | 2.04     |
| O(8)     |       | 1.32  |                     | 0.52                |                     |                     |                     |                     | 0.16 <sup>2</sup> ↓ |      |      |      | 2.00     |
| O(9)     |       |       | 1.30                | 0.11 <sup>2</sup> ↔ | 0.09                | 0.08                |                     |                     |                     |      |      |      | 1.69     |
| O(10)    |       |       | 1.39                |                     |                     |                     | 0.21                |                     |                     |      |      |      | 1.60     |
| OH       |       |       | 1.11 <sup>2</sup> ↓ |                     |                     |                     |                     |                     | 0.04 <sup>2</sup> ↓ |      |      | 0.80 | 1.95     |
| OW       |       |       |                     |                     |                     |                     |                     | 0.37 <sup>2</sup> ↓ | 0.12 <sup>2</sup> ↓ | 0.80 | 0.84 |      | 2.13     |
| $\Sigma$ | 4.98  | 5.02  | 4.91                | 2.06                | 2.03                | 2.02                | 2.03                | 2.10                | 1.04                | 1.00 | 1.00 | 1.00 |          |

\* calculated from the parameters of Brown & Altermatt (1985)

ment with mutually responsive distortions in the underlying  $[\text{Cu}_4\text{O}_{13}]$  group that shares the O(9) vertex with the tetrahedron. The following structural features allow this displacement: (1) the O(9) anion forms four weak and flexible bonds to  $\text{Cu}^{2+}$  atoms of the  $[\text{Cu}_4\text{O}_{13}]$  group; (2) the O(10) anion is coordinated by only two cation sites  $[\text{As}(3), \text{Cu}(4)]$ , and moderate flexure in the  $\text{Cu}(4)$ –O(10)–As(3) angle is allowed; (3) as mentioned above, there is considerable space around O(10), and therefore

minimal restriction is imposed on displacement of O(10); (4) the O(10) anion is the long apical ligand of the  $\text{Cu}(4)\text{O}_5$  polyhedron, stereochemically a condition that allows for considerable flexibility in the position of the O(10) atom.

For the  $\text{O}^{2-}$  anions [O(1) → O(10)], there is a reasonably strong negative correlation between anisotropy and incident bond-valence (Fig. 8). We refer to this as the “rattle” effect, whereby greater anisotropy is com-

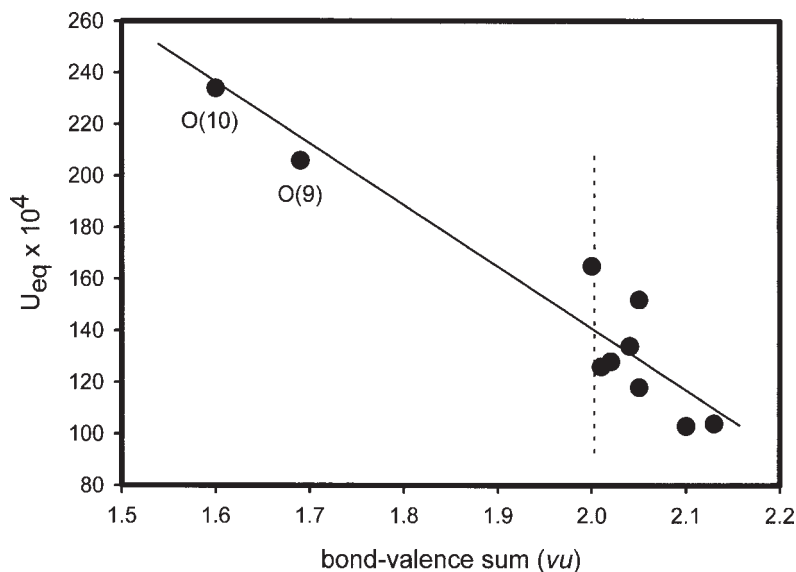


FIG. 8. The equivalent-isotropic displacements of the simple anions versus their incident bond-valence sums in the structure of andyroberrsite; the line is drawn merely as a guide to the eye.

monly associated with longer *average* bond-lengths, resulting in lower incident bond-valence sums. On a *pfu* basis, the excess bond-valence ( $>2 \text{ vu}$ ) at O(1) through O(8) is exactly offset by the deficit in bond-valence at O(9) and O(10). The mean valence for O(1)  $\rightarrow$  O(10) [ $36.09 \text{ vu} / 18 \text{ atoms of oxygen } pfu = 2.005 \text{ vu}$ ] is shown as the vertical dashed line.

What causes the large positional anisotropy associated with the  $As(3)\phi_4$  tetrahedron? Would relaxing the most anisotropic atoms off the mirror plane lead to a simple ordered arrangement with less deviant O(9) and O(10) bond-valence sums? To test this, we tried refining the structure in the space group  $P2_1$ ; however, we observed no significant departure from the  $P2_1/m$  structural model. We can therefore rule out a long-range-or-

dered lower symmetry. A more likely explanation for the anisotropy may involve chemically driven bond-length adjustments associated with extreme  $Ca \leftrightarrow Cd \leftrightarrow Mn$  chemical variations at the *M*-site (Fig. 1). The  $M\phi_6$  trigonal prism shares its O(2)–O(2) and O(5)–O(5) edges with the  $Cu(3)O_6$  and  $Cu(2)O_6$  polyhedra, respectively (Fig. 6). We can consider the  $As(3)\phi_4$  tetrahedron of the andyrobertsite structure as the weakly bonded “shock-absorber” between the strongly bonded Cu–As slabs (Fig. 5). Extreme chemical variation at the *M*-site induces positional disorder (anisotropy) in the  $[Cu_4O_{13}]$  group and the  $As(3)\phi_4$  tetrahedron. This argument suggests that the resulting atom displacements are dominantly static, rather than dynamic.

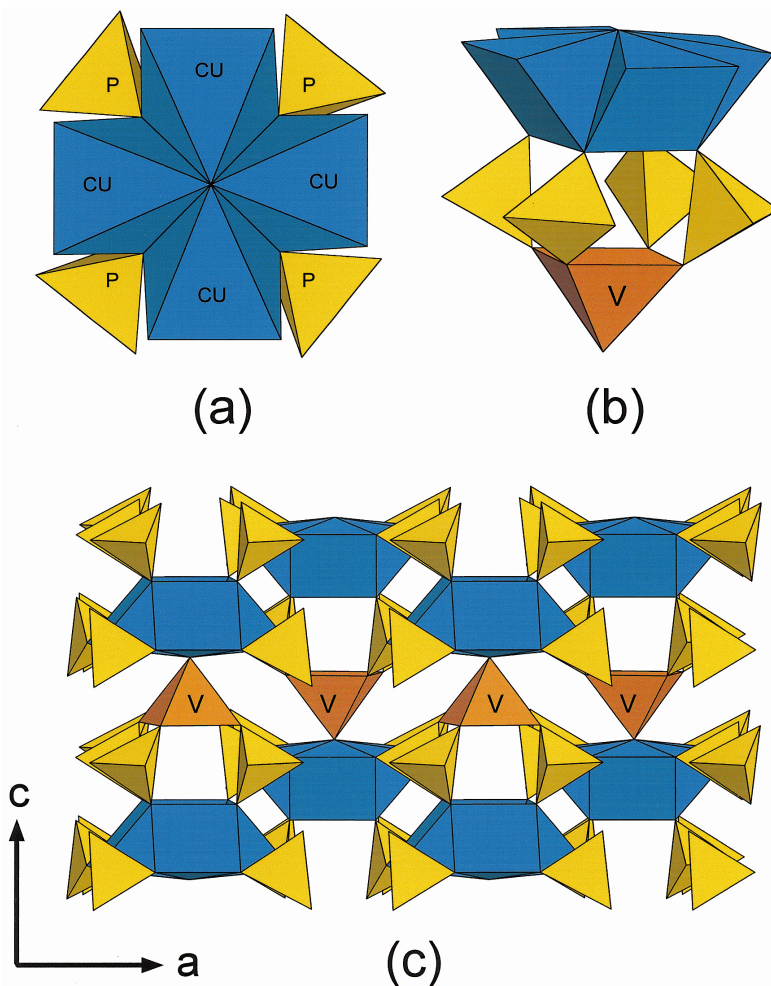


FIG. 9. The structure of  $Ba [Cu^{2+} (V^{4+}O) (PO_4)_4]$ ; (a), (b): the  $[Cu_4 (VO) (PO_4)_4 O_9]$  cluster viewed down  $[001]$  and in perspective, respectively; (c) the structural unit viewed down an axis  $4^\circ$  from  $[100]$ ; blue:  $(CuO_5)$  polyhedra; yellow:  $(PO_4)$  tetrahedron; orange:  $(VO_5)$  polyhedra.

TABLE 7. THE  $[\text{Cu}_4\text{O}_{13}]$  CLUSTER IN ANDYROBERTSITE AND  $\text{Ba} [(\text{V}^{4+}\text{O}) \text{Cu}^{2+}_4 (\text{PO}_4)_4]$ 

|   | andyrobertsite               | $\text{Ba} [(\text{V}^{4+}\text{O}) \text{Cu}^{2+}_4 (\text{PO}_4)_4]$ |
|---|------------------------------|--|
| $\langle \text{Cu}-\text{Cu} \rangle$ (Å)                     | 3.21                         | 3.20   |
| $\langle \text{Cu}-\text{O}_{\text{eq}} \rangle$ (Å)          | 1.946                        | 1.927  |
| $\langle \text{Cu}-\text{O}_{\text{ap}} \rangle$ (Å)          | 2.545                        | 2.691  |
| $\langle \text{Cu } b.v. \text{ sum} \rangle$ ( <i>vu</i> )   | 2.04                         | 2.11   |
| $\langle \text{X}-\text{O}_{\text{ap}} \rangle$ ( <i>vu</i> ) | 1.30 (X = $\text{As}^{5+}$ ) | 1.55 (X = $\text{V}^{4+}$ )  |
| $\text{O}_{\text{ap}} b.v. \text{ sum}$ ( <i>vu</i> )         | 1.69                         | 1.79   |

### Comparison with the structure of $\text{Ba} [(\text{V}^{4+}\text{O}) \text{Cu}^{2+}_4 (\text{PO}_4)_4]$

The only other occurrence of the  $[\text{Cu}_4\text{O}_{13}]$  group is in  $\text{Ba} [(\text{V}^{4+}\text{O}) \text{Cu}^{2+}_4 (\text{PO}_4)_4]$  (Meyer & Müller-Buschbaum 1997) (Fig. 9a). Phosphate tetrahedra extend from the base of the  $[\text{Cu}_4\text{O}_{13}]$  group and attach to four corners of a  $\text{V}^{4+}\text{O}_5$  polyhedron (Fig. 9b); this unit of the structure is topologically the same as the lower three-quarters of the  $[\text{Cu}_5 (\text{AsO}_4)_4 (\text{As}\phi_4) \text{O}_9]$  cluster in andyrobertsite (*cf.* Fig. 3d). Adjacent  $[\text{Cu}_4\text{O}_{13}]$  groups link *via* corner-sharing with  $\text{PO}_4$  tetrahedra in the same manner as in andyrobertsite (compare Figs. 9c and 5). The  $[\text{Cu}_4\text{O}_{13}]$  groups in adjacent Cu–P slabs are centered over one another along [001], with a direct linkage provided through the  $\text{VO}_5$  polyhedron (Fig. 9c). Hence,  $\text{Ba} [(\text{V}^{4+}\text{O}) \text{Cu}^{2+}_4 (\text{PO}_4)_4]$  contains no counterpart of the  $\text{As}(3)\phi_4$  tetrahedron in andyrobertsite. Table 7 compares several features of the  $[\text{Cu}_4\text{O}_{13}]$  group in the two structures. In both structures, the Cu–Cu distances are the same. Andyrobertsite shows slight elongation of  $\langle \text{Cu}-\text{O}_{\text{eq}} \rangle$  and concomitant shortening of  $\langle \text{Cu}-\text{O}_{\text{ap}} \rangle$ . In andyrobertsite, the apical O(9) anion bonds to  $\text{As}^{5+}$  (1.30 *vu*); in  $\text{Ba} [(\text{V}^{4+}\text{O}) \text{Cu}^{2+}_4 (\text{PO}_4)_4]$ , the analogous anion forms a short (1.622 Å) vanadyl bond to  $\text{V}^{4+}$  (1.55 *vu*) (Figs. 5, 9c). In each structure, the apical anion of the  $[\text{Cu}_4\text{O}_{13}]$  group has a low incident-bond-valence sum (1.69 *vu*: andyrobertsite; 1.79 *vu*:  $\text{Ba} [(\text{V}^{4+}\text{O}) \text{Cu}^{2+}_4 (\text{PO}_4)_4]$ ).

The anisotropic-displacement parameters for the atoms of the  $[\text{Cu}_4\text{O}_{13}]$  group in  $\text{Ba} [(\text{V}^{4+}\text{O}) \text{Cu}^{2+}_4 (\text{PO}_4)_4]$  are much more isotropic; all atoms have ( $U_{\text{max}} / U_{\text{min}}$ ) between 1 and 1.8. Of great interest is the apical anion of the  $[\text{Cu}_4\text{O}_{13}]$  group, which is isotropic [ $(U_{11} = U_{22}) = U_{33}$ ] and shows a small overall displacement ( $U_{\text{eq}} = 0.014 \text{ \AA}^2$ ). We can summarize these observations for the  $\text{Ba} [(\text{V}^{4+}\text{O}) \text{Cu}^{2+}_4 (\text{PO}_4)_4]$  structure in the following manner: (1) there is complete chemical order at all sites; (2) all sites show long-range positional order (isotropic behavior); (3) the low bond-valence sum (1.79 *vu*) at the apical anion of the  $[\text{Cu}_4\text{O}_{13}]$  group must be regarded as a characteristic feature of its very unusual stereochemistry.

We conclude that the low incident bond-valence sums in andyrobertsite and  $\text{Ba} [(\text{V}^{4+}\text{O}) \text{Cu}^{2+}_4 (\text{PO}_4)_4]$  are actual features of the structure, rather than artifacts of the structure refinement. The O(9) anion in andyrobertsite and the analogous anion in  $\text{Ba} [(\text{V}^{4+}\text{O}) \text{Cu}^{2+}_4 (\text{PO}_4)_4]$  have incident bond-valence sums of 1.69 and 1.79 *vu*, respectively, and the similarity of their coordinations indicates that these low sums must be a function of the local stereochemistry. The O(9) anion in andyrobertsite is associated with considerable surrounding anisotropic displacements, but these displacements seem to be connected to extreme substitution of differently sized cations (Ca = 1.00, Cd = 0.95,  $\text{Mn}^{2+} = 0.83 \text{ \AA}$ ) at the neighboring *M*-site. The O(10) anion in andyrobertsite (to which there is no analogue in  $\text{Ba} [(\text{V}^{4+}\text{O}) \text{Cu}^{2+}_4 (\text{PO}_4)_4]$ ) is only [2]-coordinated, with no possibility of acting as a H-bond acceptor, and again, the low incident bond-valence sum of 1.60 *vu* is the result of this connectivity. The existence of these two structures emphasizes one aspect of the valence-sum rule: in some (presumably very stable) structural arrangements, major deviations from the valence-sum rule can occur for a small number of the anions in the structure. The destabilizing effect of this feature must be outweighed by the stability of the rest of the structure. This feature is prominent also in the amphibole and pyroxene structures, where the O(4) and O(2) anions, respectively, may show major deviations (>0.25 *vu*) from the valence-sum rule.

### ACKNOWLEDGEMENTS

We thank Bill Pinch for his generosity in providing the material for this work and for his enthusiasm and encouragement. This work was supported by Natural Sciences and Engineering Research Council of Canada Research and Major Equipment Grants to FCH.

### REFERENCES

- BOUDJADA A. & GUITEL, J.C. (1981): Structure cristalline d'un orthoarséniate acide de fer(III) pentahydraté:  $\text{Fe}(\text{H}_2\text{AsO}_4)_3 \cdot 5\text{H}_2\text{O}$ . *Acta Crystallogr.* **B37**, 1402-1405.
- BROWN, I.D. & ALTERMATT, D. (1985): Bond-valence parameters obtained from a systematic analysis of the inorganic crystal structure database. *Acta Crystallogr.* **B41**, 244-247.
- BURNS, P.C. & HAWTHORNE, F.C. (1995): Coordination-geometry structural pathways in  $\text{Cu}^{2+}$  oxysalt minerals. *Can. Mineral.* **33**, 889-905.
- CHIARI, G. & FERRARIS, G. (1982): The water molecule in crystalline hydrates studied by neutron diffraction. *Acta Crystallogr.* **B38**, 2331-2341.
- COOPER, M.A., HAWTHORNE, F.C., PINCH, W.W. & GRICE, J.D. (1999): Andyrobertsite and calcioandyrobertsite: two new minerals from the Tsumeb mine, Tsumeb, Namibia. *Mineral. Rec.* **30**, 181-186.

- EBY, R.K. & HAWTHORNE, F.C. (1990): Clinoclase and the geometry of [5]-coordinated  $\text{Cu}^{2+}$  in minerals. *Acta Crystallogr.* **C46**, 2291-2294.
- FERRARIS, G. & FRANCHINI-ANGELA, M. (1972): Survey of the geometry and environment of water molecules in crystalline hydrates studied by neutron diffraction. *Acta Crystallogr.* **B28**, 3572-3583.
- \_\_\_\_\_ & IVALDI, G. (1984): X-OH and O-H...O bond lengths in protonated oxoanions. *Acta Crystallogr.* **B40**, 1-6.
- MEYER, S. & MÜLLER-BUSCHBAUM, H. (1997):  $\text{Cu}_4\text{O}_{12}$ -Baugruppen aus planeren  $\text{CuO}_4$ -Polygonen im Barium-Vanadyl-Oxocuprat(II)-phosphat  $\text{Ba}(\text{VO})\text{Cu}_4(\text{PO}_4)_4$ . *Z. Anorg. Allg. Chem.* **623**, 1693-1698.
- ONDROŠ, P., VESELOVSKÝ, F., SKÁLA, R., ČISAŘOVÁ, I., HLOUŠEK, J., FRÝDA, J., VAVŘIN, I., ČEJKA, J. & GABAŠOVÁ, A. (1997): New naturally occurring phases of secondary origin from Jáchymov (Joachimsthal). *J. Czech Geol. Soc.* **42**, 77-108.
- SCHMETZER, K. & MEDENBACH, O. (1986): Kaatialaite from Nieder-Beerbach, Odenwald – a second occurrence. *Neues Jahrb. Mineral., Monatsh.*, 337-342.

Received March 13, 2000, revised manuscript accepted June 7, 2000.